10 Mar 1991, 1:00 pm - 3:00 pm

On the Site Amplification Characteristics in San Francisco Bay Region Due to the 1989 Loma Prieta Earthquake Type Loadings

Kesuke Baba
Osaka University, Japan

Yutaka Inoue
Osaka University, Japan

Takashi Nishigaki
Konoike Corporation, Japan

Proceedings: Second International Conference on Recent Advances in Geotechnical Earthquake Engineering and Soil Dynamics, March 11-15, 1991, St. Louis, Missouri, Paper No. LP06

On the Site Amplification Characteristics in San Francisco Bay Region Due to the 1989 Loma Prieta Earthquake Type Loadings

Kesuke Baba
Architectural Engineering, Osaka University, Japan

Yutaka Inoue
Architectural Engineering, Osaka University, Japan

Takashi Nishigaki
Technical Research Institute, Konoike Corporation, Japan

SYNOPSIS A large earthquake occurred in the Santa Cruz mountains, California, on 17 October 1989, and many structures and facilities in the San Francisco Bay region suffered fatal damage from the seismic motion.
In order to evaluate the ground amplification characteristics in the region, the practical method of representing the seismic wave field may be necessary. This paper is concerned with a theoretical analysis and numerical evaluation based on the wave propagation theory to find the dynamic characteristics of the slightly sedimental basin around the San Francisco Bay due to the Loma Prieta earthquake type excitations. Numerical examples of this system are shown in the domain of frequency and time.

INTRODUCTION

Recent experimental results such as the ones in the Mexico city area (1985) and the San Francisco Bay region (1989), have let us to deliberate over the geometrical surface compositions inducing local disparities in earthquake motions, which correspond to site amplification characteristics and very large variations in great earthquake damage. A number of researches on the seismic damage in the regions have been released, and however, a few investigations of the dynamic characteristics in the site amplification phenomena have been carried out.
The present study is concerned with the dynamic analysis of a slightly alluvial and multiple layered basin standing alone on a half bedrock, and subjected to external disturbances coming from the far-field. In describing this problem with complicated boundaries, the total field is separated into the incident motion and the scattered field due to the presence of irregular boundaries. And, the latter field is further separated into the two sets of fields, corresponding to the following subproblems:
(a) one related to the imaged stratum extended flat in the horizontal direction, and
(b) the other corresponding to the difference between the scattered wave field with laterally irregular boundaries given in the original problem and the one presented in the auxiliary problem (a).
Then, the respective stress and displacement components of the auxilary problems are combined to satisfy the boundary conditions set in the original system. By applying the Fourier integral transforms in respect of time and spatial variables, the integral equations are derived in the domain of frequency and wave numbers.
In solving this equations, the response functions are expressed in terms of the unknown coefficients of the scattered displacements presented in the auxiliary problem (b).
Finally, some numerical results are shown for the physical properties obtained in the simulated systems of the San Francisco Bay region under seismic loadings.

METHOD OF ANALYSIS

Under earthquake type excitations polarized in the plane SH-field and coming from the lower far-field, the anti-plane displacement field is found in a bidimensional soil-ground which is composed of multiple layers overlying a half bedrock. Each layered medium is assumed to be perfectly elastic, and to be bounded by the free surface and the interfaces in local irregularity along the horizontal direction, the anti-plane displacement u of which satisfies the scalar Helmholtz equation in the domain of frequency,

$$(\nabla^2+k^2)u = 0, \quad k=\omega/c_s \tag{1}$$

where ω is the circular frequency of harmonic disturbances and c_s is the phase velocity of distortional waves. And, the following boundary conditions are required to be satisfied:
(i) the stress-free condition at the surface,
(ii) the continuous conditions of stress and displacement components at the interfaces.
In addition, the radiation condition in the infinite far field is required to be satisfied, which is included in the displacement representation mentioned behind.
For the brevity of this analysis, it is convenient to present the displacement field as a combination of the incident field u^i and the scattered one u^s as follows:

$$u = u^i + u^s \tag{2}$$

where the incident field is obtained in the closed form out of consideration for the irregular boundaries and the scattered one may be approximately presented in the Fourier integral transforms along the lateral direction by using the Cartesian coordinate system (x,z) in this spatial field.

$$u^s = \int_{-\infty}^{\infty} \exp(ipx) A(\tilde{x},p) Y(p)\, dp \tag{3}$$

in which $\tilde{x}$ is the position vector in the wave field and Y(p) is denoted as the unknown vector in the domain of wave number p. When the wave field associated with the irregularly layered system is completely described, it should contain any component expanded along an arbitrary direction. The scattered displacement representation of the equation (3), however, has only the components in the domain of laterally expanded wave number, and in addition to that, the scattered field in the half bedrock is restricted to giving up incoming components so as to introduce the aberration named Rayleigh ansatz error, which is practically small when the geometrical irregularity in the interfaces is slight and the incident waves have only low frequency components.
By using Eqs. (2), (3) in the boundary conditions, the following equation associated with the unknown functions Y(p) is obtained,

$$\int_{-\infty}^{\infty}\exp(ipx)\,G(\tilde{x}_c,p)\,Y(p)\,dp = \exp(-ikx)\,h(\tilde{x}_c) \qquad (4)$$

where the position vector of the irregular boundaries is denoted by $\tilde{x}_c$ in the unique expression of the horizontal coordinate x, and k is the lateral component of the incident distortional wave number when incoming turbulences are propagating obliquely.
In order to derive the boundary equation in the domain of wave numbers, the Fourier transform in respect of the horizontal coordinate is to be applied to Eq. (4) with the following restriction on the boundary configuration in the lateral direction so that the transform containing infinite integrals is convergent,
(A) the irregular zone $|x|\leq L$ which includes the irregular boundaries in the local portion of multiple layers, and
(B) the regular zone $|x|>L$ which is composed of the multiple layers extended flat in the lateral direction.
In addition, the auxiliary problem (a) mentioned previously is considered, which corresponds to the imaged half-space having the multiple flat-layers in consistence with the objective ones within the regular zone and its solution presented in the domain of wave number is given by using the Dirac's delta function,

$$Y_0(p) = \delta(p+k)\,G_0^{-1}(p)\,h_0 \qquad (5)$$

the coefficients of which hold the following relationships with the ones in the original boundary equation (4),

$$\begin{aligned} G(\tilde{x}_c,p) &= G_0(p) \\ h(\tilde{x}_c) &= h_0 \end{aligned} \qquad :|x|>L \qquad (6)$$

By making use of the solution of the subproblem and the relations in the coefficients, the boundary equation (4) is reconstructed in respect of the functions $Y_1(p)$, which are the difference between the functions Y(p) associated with the original problem and $Y_0(p)$ in the auxiliary problem,

$$Y_1(p) = Y(p) - Y_0(p) \qquad (7)$$

and transformed in the Fourier integrals along the horizontal direction with the exchange in the order of the double integrals, which are found in the scattered terms of the transformed boundary equation. The equation associated with the unknown functions $Y_1(p)$ may yield the following integral equations in the domain of wave numbers p and q:

$$G_0(q)Y_1(q)+\int_{-\infty}^{\infty}[K_1(p,q)-K_2(p,q)]\,Y_1(p)\,dp = f_1(q)-f_2(q) \qquad (8)$$

in which the coefficients are obtained in the finite integral forms as follows:

$$\begin{bmatrix}K_1(p,q)\\K_2(p,q)\end{bmatrix} = \frac{1}{2\pi}\int_{-L}^{L}\exp\{-i(q-p)x\}\begin{bmatrix}G(\tilde{x}_c,p)\\G_0(p)\end{bmatrix}dx \qquad (9)$$

$$\begin{bmatrix}f_1(q)\\f_2(q)\end{bmatrix} = \frac{1}{2\pi}\int_{-L}^{L}\exp\{-i(q+k)x\}\begin{bmatrix}h(\tilde{x}_c)\\G(\tilde{x}_c,-k)\,G_0^{-1}(-k)\,h_0\end{bmatrix}dx$$

Furthermore, the coefficients can be expressed analytically when the heterogeneous boundaries in the irregular zone are in the composition of piecewise linearized planes.
The frequency transfer function $U(\tilde{x})$ of this irregularly layered ground due to seismic waves are expressed in terms of the solutions $Y_1(p)$ which are obtained in the numerical analysis of the integral equations (8).

$$U(\tilde{x}) = U^{i}(\tilde{x})+\exp(-ikx)\,A(\tilde{x},-k)\,G_0^{-1}(-k)\,h_0 + \int_{-\infty}^{\infty}\exp(ipx)\,A(\tilde{x},p)\,Y_1(p)\,dp \qquad (10)$$

Consequently, the response functions in the domain of frequency or time are presented in the product of the transfer functions and the spectra of external loadings, or in its Fourier inverse transforms in respect of frequency parameters.

APPLICATION TO THE SIMULATED GROUND MOTION IN THE BAY REGION

On 17 October 1989, a large earthquake (m_b=6.9, M_s=7.1) occurred near Loma Prieta Observatory in the Santa Cruz Mountains, approximately 16 kilometers northeast of the city of Santa Cruz, California, as shown in Fig. 1.
The rupture began at 37°04' North, 121°88' West, and was running in the direction of North 50° West with the depth of about 18 kilometers, the dip of 70° and the rake of 130° along the San Andreas fault, typical earthquake on which are the result of the horizontal slip of the ground on the two sides of the fault, with the southwest side moving northwest and thrusting up and over the northeast side relative to the northeast side due to the tectonic stress.
The focal mechanism of the Loma Prieta earthquake is presented in Fig. 2 by using the fault-plane solution in the study of U.S. Geological Survey.

Around the San Francisco Bay, a large number of structures and transportation facilities situated on the soft alluvium suffered heavy damage from the seismic motion. In order to evaluate the typical site amplification characteristics in the San Francisco Bay region under earthquake type loadings, the simulated ground motion is analyzed on the section S-S' across the Bay, as drawn in Fig. 1. The section is running from Sky Londa to Coyote Hills and its location is at a distance over 30 kilometers from the epicenter of the Loma Prieta earthquake. When the seismic waves propagate with the pure shearing-force normal to the section, the major components in the wave field may be the anti-plane ones. In this idealized case, the analytical method mentioned previously can be applied to the bidimensional ground motion on the vertical plane of the section S-S'.
The geological materials of the alluvial basin in the Bay region are complicated and irregularly accumulated, and the typical properties are shown as:

1) BAY MUD is unconsolidated, water-saturated and plastic carbonaceous clay and silty clay,
2) HOLOCENE ALLUVIUM is unconsolidated, moderately sorted and permeable sand and silt with coarse sand and gravel,
3) LATE PLEISTOCENE ALLUVIUM is weakly consolidated, slightly weathered, poorly sorted and irregularly interbedded clay, silt, sand and gravel,
4) PLEISTOCENE BEACH AND DUNE SAND DEPOSIT is loose, well-sorted and fine to medium sand,
5) EARLY PLEISTOCENE ALLUVIUM is moderately consolidated, deeply weathered, poorly sorted and irregularly interbedded clay, silt, sand and gravel,
6) PRE-TERTIARY AND TERTIARY BEDROCK is stable and called Franciscan Formation.

In the construction of the layered model for fitting the analytical procedure, the complicated alluvial deposits are simplified, as shown in Fig. 3, which are composed of four layers having irregular and piecewise linearized boundaries. The shearing velocity and the maximum depth of each layer are presented in Table 1. The cross section of the multiple layered basin surrounded by the bedrock has the geographical configuration of 26 kilometers width and 180 meters depth, and the proportional ratio in the vertical section is very slight as 0.18/26=0.00692.
By the way, no matter how slight the basin standing alone on a half basis is, it is not difficult to construct the dynamic system due to seismic loadings as far as the method prepared in this paper is put in use, which is capable to introduce analytically the configuration of irregular boundaries in the laterally finite region into the formulation.
In simulating the dynamic characteristics in the site amplification behavior of the San Francisco Bay region due to the Loma Prieta earthquake type loadings, the transfer functions are evaluated on the first step of this analysis, which are accompanied by the multiple layered alluvium with the piecewise linearized irregular boundaries shown in Fig. 3, under vertically polarized incident waves propagating through geologically various and long paths from the epicenter, and in the combination with the transfer functions, the dynamic response

Table 1.
Simplified geologic properties in the San Francisco Bay region, followed by the data of USGS.

	Depth	Materials	S-wave velocities
I	30 m	Silty clay	54 m/sec
II	60	Sandy clay	180
III	180	Sand	318
IV	∞	Rock	1,510

functions on the surface of the basin which is subjected to the earthquake type excitations incoming from the lower far-field, is studied in the domain of frequency and time on its second step. Finally, the distributions of the response functions in the simulated systems are discussed with the evaluation of the seismic damage suffered from the real earthquake in the San Francisco Bay region.

NUMERICAL ANALYSIS AND CONCLUDING REMARKS

In order to analyze the dynamic ground motions on a slightly alluvial basin setting alone on a half basis, it is assumed that the bidimensional and anti-plane wave field is presented in a multiple layered half-space with piecewise linearized heterogeneous boundaries in the irregular zone $|x| \leq L$, and negligibly thin and horizontally flat surface layers in the regular zone $|x| > L$ where the bedrock is assumed to appear nakedly. And the soil ground is composed of the linear hysteretic type viscoelastic medium whose generalized Lame's constants are expressed mathematically in complex forms as its phase velocities are shown:

$$C_j = C_{j0}(1+iD_j) \qquad :j=1,2,3,4$$

in which C_{j0} and D_j are the real part and the viscose damping ratio in the phase velocity of the layered medium (j).
In the numerical analysis of the systems, the infinite integral equations (8) in respect of the unknown coefficients expressed in the auxiliary problems are converted into the simultaneous equations by means of the discretization and truncation technique in the domain of wave numbers as well as the transfer functions (10) are derived in the finite summations. For the calculation carried out in general forms, the dimensionless parameters and dimensionless components in the physical properties of the systems are introduced with the superscript ($\bar{}$) as:

$$\bar{x}=x/L, \quad \bar{z}=z/L, \quad \bar{p}=pL, \quad \bar{q}=qL, \quad \bar{k}=kL,$$

$$\bar{\omega}=\omega L/C_0, \quad \bar{t}=tC_0/L, \quad \bar{C}_j=C_j/C_0,$$

$$\bar{u}=u/|u^i|$$

in which L is the half width of the basin and C_0 is the standard phase velocity. In the integration and summation to obtain the responses in the domain of frequency and time according to Eqs. (8) and (10), there are no singularities because of the elimination of the infinitely travelling waves along the horizontal direction in the application of the auxiliary problem associated with the flat-layered ground and the presence of the dissipative damping in the soil layer. Therefore ordinary methods of computation can be made while an appropriate interpolation technique is necessary in evaluating the discretized and truncated functions.

In this analysis, the following numerical values of the standard and dimensionless parameters for the ground systems are chosen as:

$$L=13{,}000 \text{ (m)}, \quad C_0=1{,}510 \text{ (m/sec)},$$

$$D_j=0.01 \quad : j=1\sim4$$

and the east edge in the surface of the alluvium is situated at $\bar{x}=1$ and the west one is at $\bar{x}=-1$. The amplification factors at the various points on the surface of the deposit due to vertically incident excitations are presented in frequency domain, as shown in Fig. 4.

The violently amplified portions found in $\bar{\omega}>15$ are concentrated within the top alluvium (I) which is localized in the central region of the basin $|\bar{x}|<0.5$ and modeled as the composition of the Bay Mud and Holocene Alluvium, and at the other positions on the surface they exhibit almost quite slight values.

In Fig. 5, the amplification factors distributed on the surface of the multiple layered ground are presented at some incident frequency levels. The factors exceeding ten times are indicated in the frequency range over $\bar{\omega}=20$ inside the soft alluvium (I). For the research in the locarized prominence of the amplification factors appeared on the alluvium (I) in comparison with the more simplified case, the double layered soil ground under vertical loadings is considered, which is assumed to be composed of the half-spaced bedrock and the surface layer having the geological property of the alluvium (III) and spreading over the composite regions of the layers (I), (II) and (III) as shown in Fig. 6. In the simplified case associated with the double layered system, the prominant behavior of the amplification factors is found all over the surface of the sediment in Fig. 7.

By comparing the amplified characteristics of both multiple and simply double layered systems, it is noted that the soft and locarized sediment standing on the surface of the multiple layers is obliged to accept the concentrated seismic violence.

The dynamic behavior of the multiple layered alluvium simulated in the Bay region is presented in time domain as found in Fig. 8, which is assumed to be subjected to the idealized transient waves of the Ricker wavelet type with the central spectrum of $\bar{\omega}_c=10$ and little contribution in high frequency range, and as shown in Fig. 9 under a part of the horizontal components in the real Loma Prieta earthquake obserbed on the hard bedrock inside the location of University of California, Santa Cruz. In these figures of time histories, the prolongation of the wave propagating duration is appeared especially within the top alluvium (I) composed of geologically soft materials. So tha the surface sediment localized on the multiple layers is excited much more long time than the ground outside it.

Finally, it is concluded that, in spite of the rough analysis in this paper, the site amplifie behavior of the irregularly and multiple layere ground systems is well accounted in the qualitative characteristics for the disastrous distributions which are concentrated strongly on the localized surface deposit composed of the Bay Mud and the other soft materials in the San Francisco Bay region suffered from the Loma Prieta earthquake.

REFERENCES

Aki, K. and K.L. Larner (1970) Surface motion o a layered medium having an irregular interface due to incident plane SH waves. J. Geophys. Res., 75, 933-954.

Bard, P.Y. and M. Bouchon (1980) The seismic response of sediment-filled valleys, Part I and II. Bull. Seism. Soc. Am., 70, 1263-1286 1921-1941.

Baba, K., Y. Inoue and T. Nishigaki (1988) Dynamical behavior of a slightly alluvial basin due to plane wave turbulences. 9WCEE, II, 689-694.

USGS (1989) U.S. Geological survey strong-motior records from the northern California (Loma Prieta) earthquake of October 17, 1989. Geological survey open-file report 89-568.

CDMG (California Department of Conservation, Division of Mines and Geology, Office of Strong Motion Studies) (1989) CSMIP strong-motion records from the Santa Cruz Mountains (Loma Prieta), California earthquake of 17 October 1989.

Building Research Institute, Ministry of Construction in Japan and Tokyo Soil Research Corp. (1989) Loma Prieta Earthquake Oct. 17, 1989, Reconnaissance Report.

Japanese Group for the Study of National Disaster Science (1990) Loma Prieta Earthquak of October 17, 1989, Reconnaissance Report. National Disasters Research Report, No. B-1-3

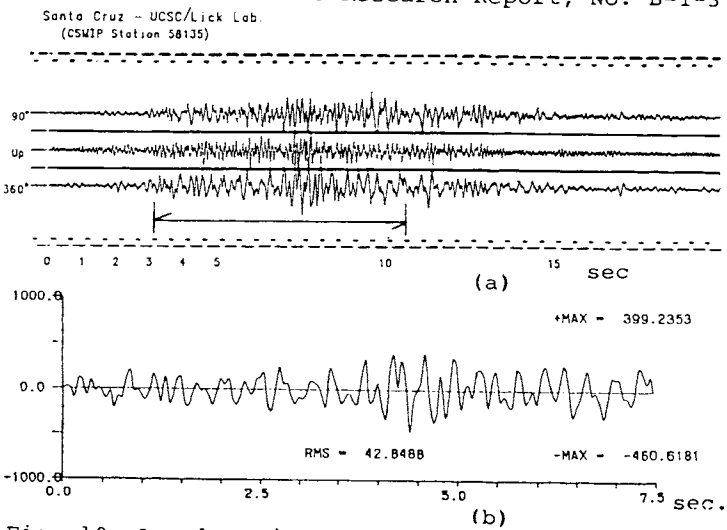

Fig. 10 Acceleration records of the Loma Prieta earthquake obserbed in UCSC, Santa Cruz. The indicated part in (a) which is zoomed up in (b) is used for the analysis in Fig. 9.

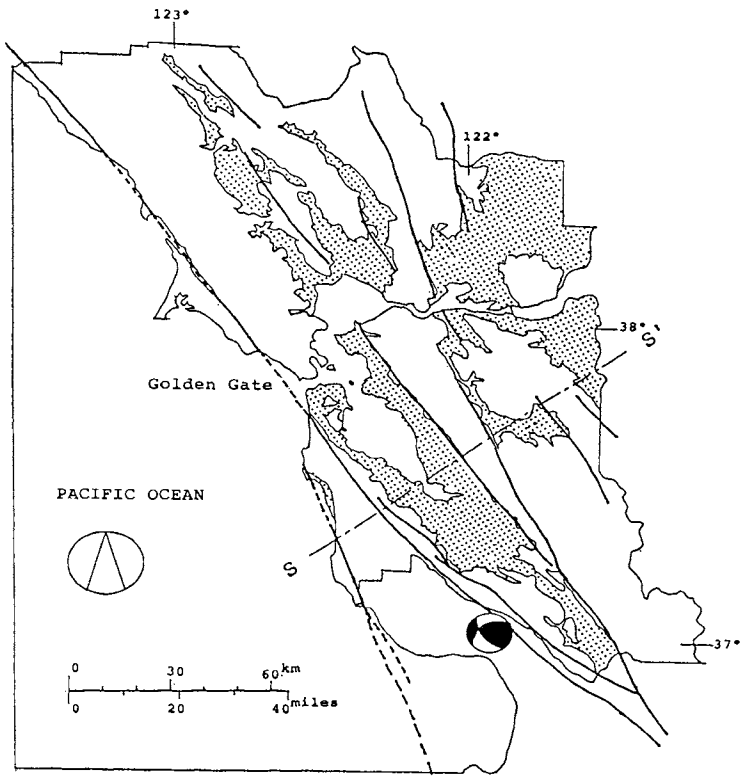

Fig. 1 Geologic map of the San Francisco Bay region. dotted areas: soft deposits, solid lines: branches of fault system, S-S': the horizontal line in the cross section presented in Fig. 3.

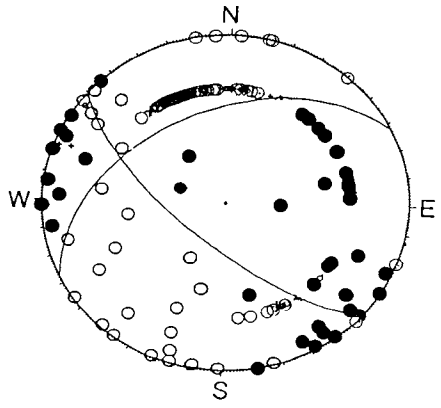

Fig. 2 Lower hemisphere, projection of fault plane solutions of the Loma Prieta main shock, followed by the research of USGS, 1989. open circles: tensions, solid circles: compressions.

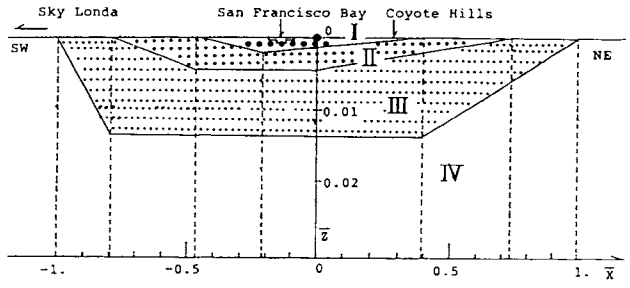

Fig. 3 Geologic cross section of the modified San Francisco Bay region.

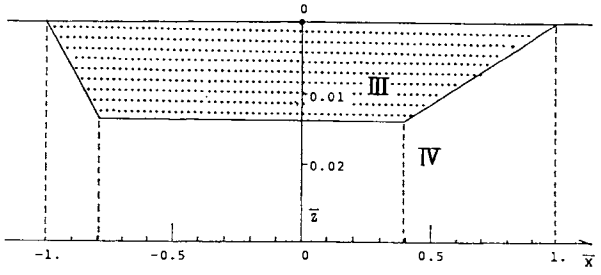

Fig. 6 Geologic cross section of the double layered ground, which is constructed in the simplified configuration of Fig. 3.

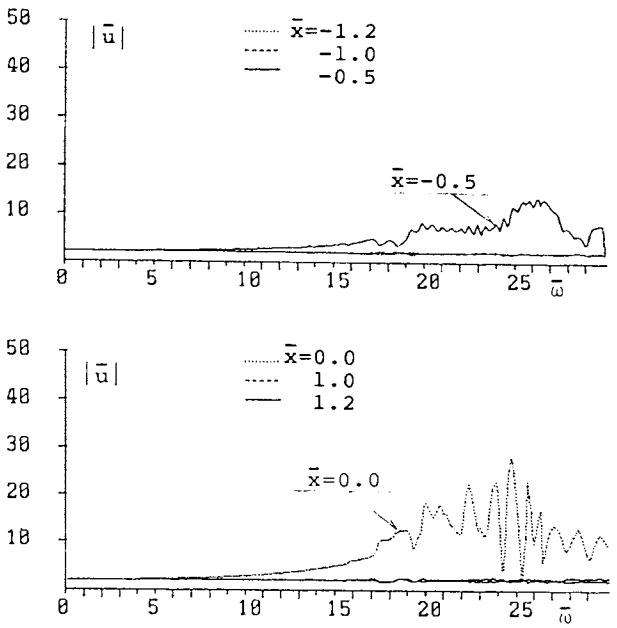

Fig. 4 Amplification factors on the multi-layered ground surface due to vertically incident waves in frequency domain.

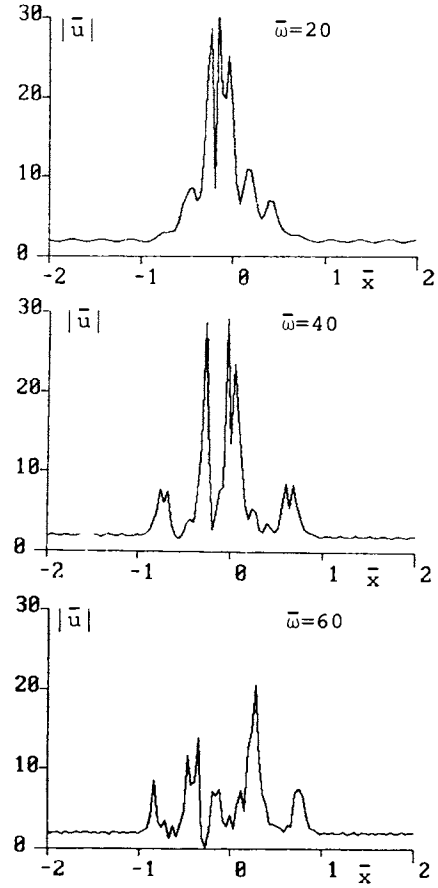

Fig. 5 Amplification factors distributed on the multi-layered ground surface due to vertically incident waves.

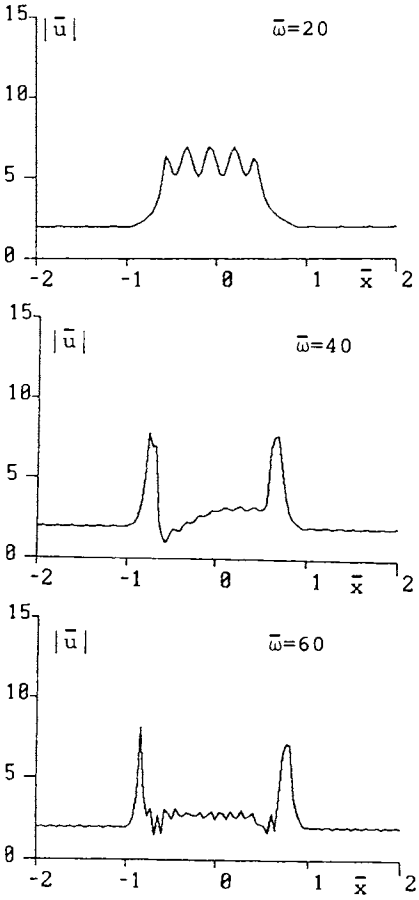

Fig. 7 Amplification factors distributed on the double layered ground surface due to vertically incident waves.

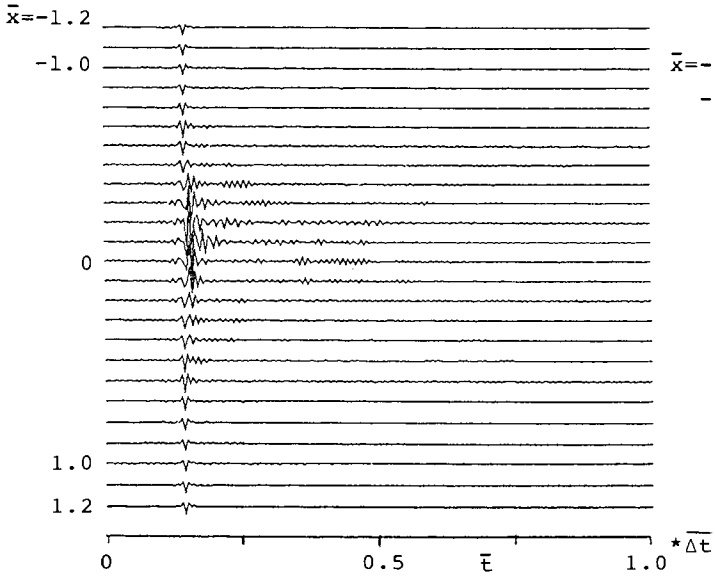

Fig. 8 Time histories of displacement responses on the multi-layered ground surface under the Ricker wavelet of $\bar{\omega}_c$=10. $\bar{\Delta t}$=21.14

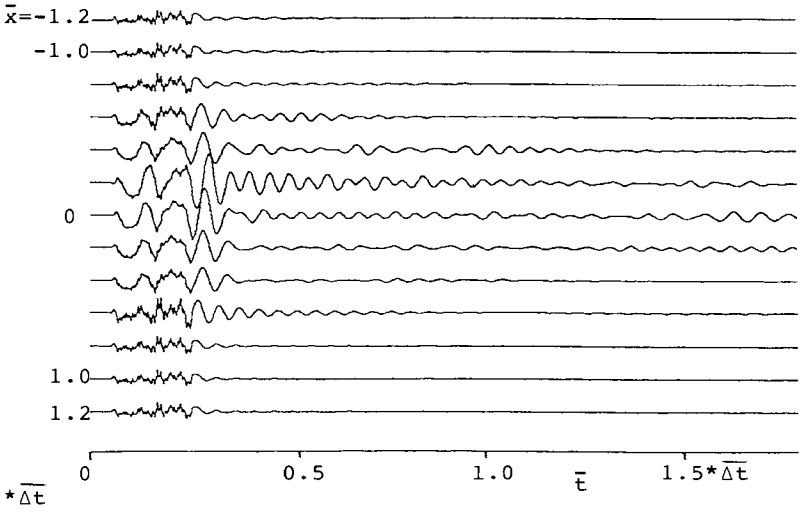

Fig. 9 Time histories of displacement responses on the multi-layered ground surface under a part of the Loma Prieta main shock (about 7.5 sec) obserbed in UCSC, Santa Cruz. $\bar{\Delta t}$=4.06

Proceedings: Second International Conference on Recent Advances in Geotechnical Earthquake Engineering and Soil Dynamics, March 11-15, 1991, St. Louis, Missouri, Paper No. LP07

Performance of a Pile-Supported Structure under Strong Ground Motion

Phillip L. Gould
Professor of Civil Engineering, Washington Univ., St. Louis, MO

Kijun Ahn
Graduate Student, Washington Univ., St. Louis, MO

SYNOPSIS : The influence of soil-pile-structure interaction on the response of a mid-rise reinforced concrete structure to the Loma Prieta earthquake was investigated. Because earthquake ground motion has relatively high frequency content, lengthening the period of a structure has the effect of reducing the inertia forces. A pile foundation tends to lengthen the period through the soil-pile-structure interaction mechanism.

The seismic response of the Clarion Hotel was studied in detail for five different base conditions. As an initial estimate of the importance of the interaction effects, a free vibration analysis was carried out. The flexible base model results in an increase in the natural period of the system and corresponding reduction in the base acceleration. A nonlinear time history analysis was carried out, and the calculated forces and the displacement in the building and the pile are compared for different base conditions.

INTRODUCTION

The concept of isolating a building from earthquake effects by lengthening the natural period of the building is well understood. Since earthquake ground motion has relatively high frequency content, lengthening the natural period has the effect of reducing the inertia forces. The pile foundation may play the role of a base isolator under earthquake loading through the mechanism of soil-pile-structure interaction. During the soil-pile-structure interaction, the base of the structure can translate or rotate and a substantial amount of the vibrational energy of the structure can be dissipated through the soil medium by hysteretic and radiation damping, which change the dynamic characteristics of the structure compared with a fixed base structure.

To obtain realistic responses for soil-pile-structure systems, the analysis must include variations of soil properties with depth, nonlinear stress-strain relationships of soils, and variations of free-field soil deformation with depth. A versatile method of analysis which permits the inclusion of all these factors without requiring a voluminous computation is not yet developed.

Approaches based on the beam-on-Winkler-foundation model are widely used for the analysis and design of single piles subjected to static lateral loads. While current state-of-the-art procedures for static analysis are mostly semi-empirical, established methods for dynamic analysis are theoretically based. A type of Winkler model uses pile force-displacement (p-y) curves to describe the deformation characteristics of the soil based on field load tests. This model consists of nonlinear springs and dashpots placed in parallel. The spring constant is defined by the p-y curves which describe the material nonlinearity of the soil, and the dashpot constant is defined from the hysteretic and the radiation damping of the soil. In this work, a p-y curve is utilized to treat the material nonlinearity of the soil. The pile is modeled by beam-column elements which have material and geometric nonlinearities.

A free vibration analysis and a nonlinear time history analysis were carried out to investigate the effects of soil-pile-structure interaction on the seismic response of the Clarion Hotel near the San Francisco International Airport. The nonlinear shear modulus for the soil springs was defined utilizing a p-y curve, q-z curve, and t-z curve for horizontal, vertical and pile tip springs, respectively.

GENERAL FORMULATION FOR THE SOIL-PILE-STRUCTURE INTERACTION

The most popular schemes for the solution of nonlinear finite element equations are some form of Newton-Raphson iteration. In this study the modified Newton-Raphson iteration method is used. For a structure supported on a pile foundation, the governing equations at time $t+\Delta t$ can be written in matrix form as:

$$\begin{bmatrix} M_{ss} & M_{sp} \\ M_{ps} & M_{pp} \end{bmatrix} \begin{Bmatrix} \ddot{U}_s \\ \ddot{U}_p \end{Bmatrix}^{(k)}_{t+\Delta t} + \begin{bmatrix} C_{ss} & C_{sp} \\ C_{ps} & C_{pp} \end{bmatrix} \begin{Bmatrix} \dot{U}_s \\ \dot{U}_p \end{Bmatrix}^{(k)}_{t+\Delta t} + \begin{bmatrix} K_{ss} & K_{sp} \\ K_{ps} & K_{pp} \end{bmatrix} \begin{Bmatrix} \Delta U_s \\ \Delta U_p \end{Bmatrix}^{(k)}_{t+\Delta t} \quad (1)$$

$$= \begin{bmatrix} M_{ss} & M_{sp} \\ M_{ps} & M_{pp} \end{bmatrix} \{T\} \ddot{Z}_{g_{t+\Delta t}} - \begin{Bmatrix} F_s \\ F_p \end{Bmatrix}^{(k-1)}_{t+\Delta t}$$

in which the subscripts i,j = s indicates nodes above the superstructure-pile interface, while i,j = p refers to nodes at the pile segments ; $\ddot{Z}_g$ denotes the ground acceleration; T is the transformation vector for $\ddot{Z}_g$ to be applied to the

corresponding components of degree of freedom of the system; $\{U_i\}^{(k)}$ and $\{U_i\}^{(k)}$ are the vectors of nodal point velocities and accelerations in iteration k ; $\{F_i\}^{(k-1)}$ is the vector of nodal point forces corresponding to the internal element stresses in iteration $k-1$.

The total displacement at time $t+\Delta t$ is obtained by adding the incremental displacement to the displacement at the previous time t:

$$\begin{Bmatrix} U_s \\ U_p \end{Bmatrix}^{(k)}_{t+\Delta t} = \begin{Bmatrix} U_s \\ U_p \end{Bmatrix}^{(k-1)}_{t+\Delta t} + \begin{Bmatrix} \Delta U_s \\ \Delta U_p \end{Bmatrix}^{(k)} ; \quad \begin{Bmatrix} U_s \\ U_p \end{Bmatrix}^{(0)}_{t+\Delta t} = \begin{Bmatrix} U_s \\ U_p \end{Bmatrix}_t \quad (2)$$

where $\{\Delta U_i\}^{(k)}$ is the vector of nodal point incremental displacements in iteration k.

The tangent stiffness matrix of the system is a assemblage of submatrices which are the linear stiffness matrix of the structure, $[K_{ss}]$, and the summation of the stiffness matrices of the pile and the soil,

$$[K_{pp}] = [K]_{pile} + [K]_{soil} \quad (3)$$

The damping matrix of the system can be assembled similarly to the stiffness matrix of the system. The damping matrix of the soil is added to the damping matrix of the pile as

$$[C_{pp}] = [C]_{pile} + [C]_{soil} \quad (4)$$

SOIL CHARACTERIZATION

Soil Stiffness

One of the important factors in the analysis of interactive pile behavior is the constitutive law for the soil. The relationships between the stresses and the strains of the soil are much more complicated than the simple, linearly elastic moduli. Therefore, some form of nonlinear relation must be used to represent the soil. In this study a modified Romberg-Osgood model is employed to represent the soil resistance-displacement curves:

$$P = P_c + \frac{K_h(y-y_c)}{\left[1+\left(\frac{1}{C}\left|\frac{k_h(y-y_c)}{P_u}\right|\right)^n\right]^{1/n}} \quad (5)$$

where

$$C = \left| \pm 1 - \frac{P_c}{P_u} \right| \quad (6)$$

and k_h = initial lateral stiffness of the soil; P = generalized soil resistance ; P_u = ultimate lateral soil resistance; n = shape parameter; y = generalized displacement; P_c = soil resistance at the previous reversal; and y_c = soil displacement at the previous reversal.

The expression for the tangent modulus is obtained by differentiating equation (5) with respect to displacement y.

Soil Hysteretic Damping

To represent the damping characteristics of the soil resulting from the deformations produced by interaction with the pile, nonlinear viscous dashpots are employed. For the damping ratio of the soil dashpots, the simple relationship between the shear modulus and damping which was derived by Hardin and Drnevich (1972) is utilized:

$$D = D_{max}\left(1 - \frac{G}{G_{max}}\right) \quad (7)$$

Replacing G and G_{max} by the soil spring coefficients k_{ht} and k_h and utilizing the critical damping coefficient from Richart et. al., the coefficient of hysteretic damping of the soil can be obtained as

$$C_{soil} = 2\,D_{max}\left(1 - \frac{k_{ht}}{k_h}\right)\sqrt{k_{ht}\,m} \quad (8)$$

where k_{ht} is the tangent modulus of the soil and m is the pile mass per unit length.

Soil Radiation Damping

Assuming that a horizontally moving pile cross section would generate solely 1-D P-waves travelling in the direction of shaking and 1-D SH-waves in the direction perpendicular to shaking, the coefficient of the one-dimensional viscous dashpot that will absorb the energy of the waves originating at the soil-pile interface can be written as:

$$C = 2\rho A V_s\left[1 + \frac{V_p}{V_s}\right] \quad (9)$$

$$V_p = V_s\left[\frac{2(1-\nu)}{1-2\nu}\right]^{1/2} \quad (10)$$

where V_p and V_s are P-wave and S-wave velocities, respectively. The use of V_p as an approximate wave velocity in the compression-extension zone generates a singularity when Poisson's ratio, ν, approaches 0.5. In order to remove this singularity, Lysmer's analog "wave velocity" is used instead of V_p:

$$V_{La} = \frac{3.4\,V_s}{\pi(1-\nu)} \quad (11)$$

Because the absorption characteristics of this boundary are frequency independent, the boundary can absorb both harmonic and nonharmonic waves.

BUILDING MODEL

The Clarion Hotel consists of four building units connected by friction joint systems (Figure 1). For this project, Tower I was selected to be analyzed (Figure 2). Since the building is more rigid in the NW-SE direction, the NE-SW is chosen as the direction of earthquake loading. The building has four shear walls in the NW-SE direction and the floor slabs are reinforced concrete flat plates. The connection between the shear walls and the slab is conventional cast-in-place construction. The building was modeled using both a 2-D frame-shear wall model and a simplified, stick model (Figure 3 and 4). For the simplified stick model, a beam-column element is used. The geometric properties of the element were computed based on the gross sections of the walls and columns, and the mass of each floor is added to the nodal point of the beam-column element as a lumped mass. Rotational springs are attached to nodal points to represent the bending moment resistance from the floor slab. Based on the good correlation between periods for the frame-shear wall model and the simplified stick model, the simplified stick model is used for the remaining analysis.

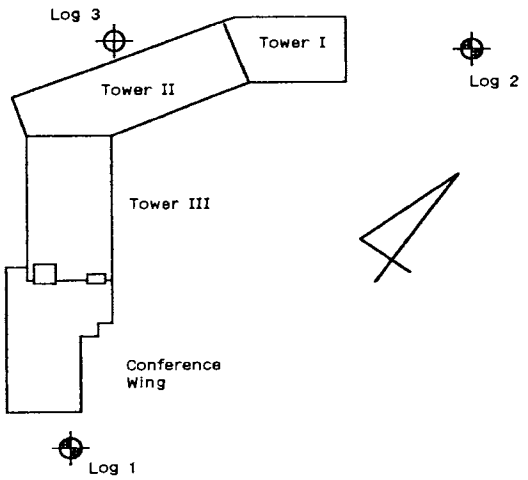

Figure 1. Airport Plaza Hotel and Boring Locations

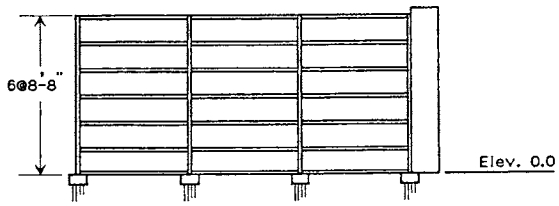

Figure 2a. Elevation of Tower I of Airpott Plaza Hotel

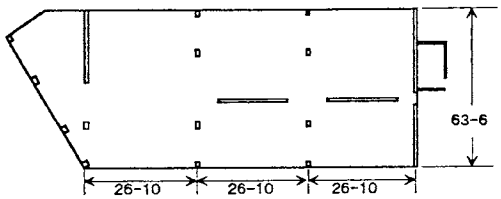

Figure 2b. Floor Plan of Tower I of Airport Plaza Hotel

GROUND CONDITION

The Hotel is supported on a pile foundation penetrating into the stiff, clayey soils underlying the soft Bay Mud layer. The site is reclaimed tide land of San Francisco Bay that was filled with loose to medium dense silty to clayey sand about four to six feet thick. A characteristic site period was estimated based on a depth to bed rock of 200 feet and established correlations between undrained shear strength and shear modulus. Using the equivalent single-layer method (UBC 1979), the characteristic site period was estimated to be of the order of 0.8 to 1.0 second.

Since the actual soil profile directly underneath the building is not available, the soil profile is approximated using the data from three exploratory borings drilled at the location as shown in Figure 1. The interpolated soil profile is shown in Figure 5. The soil properties also reflect the available data from the laboratory tests of the soil samples obtained from the borings, and shown in Table 1.

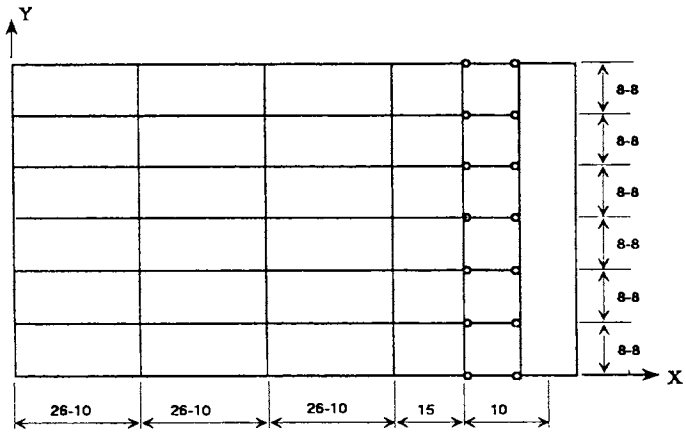

Figure 3. 2-D Frame-Shear Wall Model

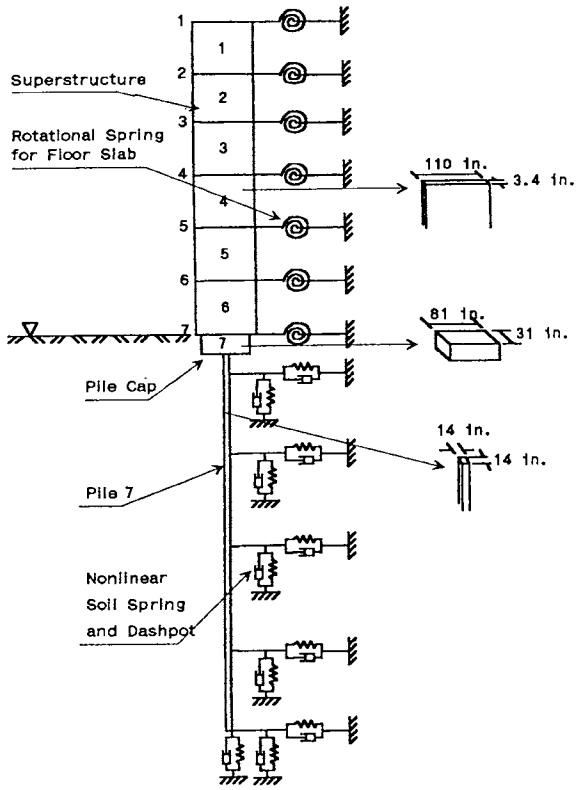

Figure 4. The Simplified Stick Model

SOIL-PILE-STRUCTURE MODEL

Since the soil spring coefficients in the p-y curves are dependent upon the pile cross section, the composite model pile is chosen to have the size of the pile used for the Hotel. In order to obtain the corresponding cross section of the superstructure for the stick model, the foundation stiffness is obtained by first considering the pile group factor. Then the scaling factor is calculated by dividing the foundation stiffness by the stiffness of the model pile. The cross section of the building for the stick model is found similarly, dividing the gross section of walls and columns by the scaling factor. Figure 4 shows the cross

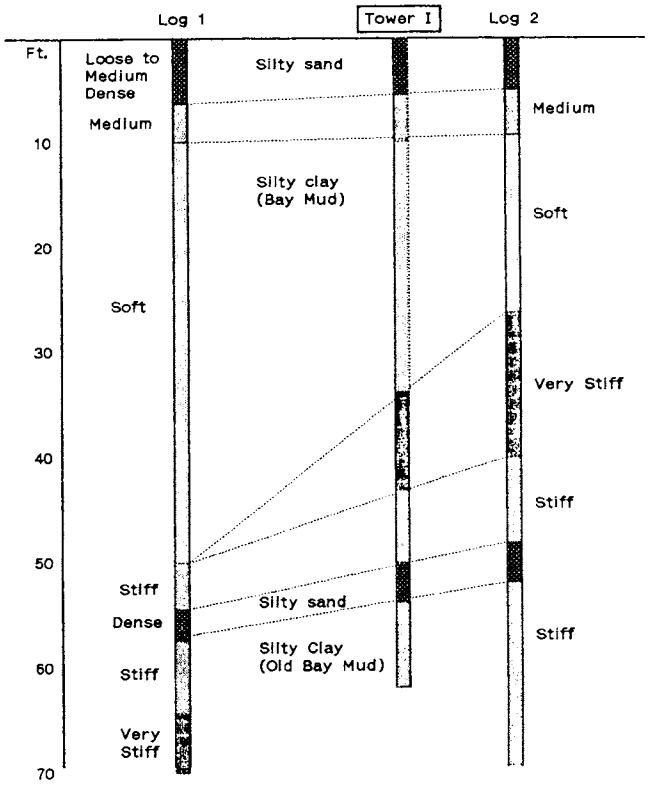

Figure 5. The Interpolated Soil Profile underneath Tower I

sections of the superstructure, the pile cap, and the pile for the stick model.

A rotational spring is attached at the base node to represent the rotational resistance provided by the foundation slab and the pile foundation. The foundation slab was cast-on-grade and spans from pile cap to pile cap. When the foundation slab is assumed to be rigid, the rotational resistance can be calculated from the geometry of the pile foundation. However, due to the limited capability of the computer program and uncertainties regarding the soil properties and the connection between the slab and the pile cap, four different coefficients are used for the rotational spring attached at the base. These are designated as R1~R4. For each case, the rotational stiffness of the floor slab for each bay is first calculated, and then they are summed together for the base floor stiffness. The coefficient of the rotational spring is then obtained by dividing the rotational stiffness of the base floor by the scaling factor.

ANALYSIS RESULTS

Free vibration is carried out for five different base conditions, the non-interactive fixed base case and the four spring restrained cases mentioned in the previous section. The increase in rotational stiffness corresponds to increased bending resistance of the floor slab between pile heads. In this stick model, the translational stiffness of the pile is the same for all four cases; only the rotational stiffness at the pile head increases.

Table 1. The soil properties

	Dry Density (pcf)	Moisture Content (%)	Penetration Blow Count N	C_u	α
Silty sand	101	20.8	8		
	50	85	13	1375	0.63
Silty Clay	50	85	1	211	1.08
	112	18	24	2442	0.4
	80	60	13	1375	0.63
Silty Sand	130	18	26		
Silty Clay	66	60	13	1375	0.63

Soft clay
Medium clay
Stiff clay
Loose to medium sand
Dense sand

Table 2 presents the natural frequencies for the first three modes. For the fixed base case, the computed fundamental period is 0.347 second for the stick model. The fundamental period of the 2-D frame-shear wall model is 0.286 second and the approximated period from the UBC formula is 0.387 second. As shown in the Table 2, the fundamental period increases as the rotational stiffness at the pile head decreases. It is very interesting to note that the frequencies of the second and the third mode are almost the same for all four cases.

Table 2 Fundamental Frequencies of the First Three Modes and Natural Periods

	1st Mode	2nd Mode	3rd Mode	Period(sec.)
Fixed	2.878	17.223	25.223	0.347
R1	2.457	6.278	14.472	0.407
R2	1.963	6.274	14.472	0.509
R3	1.106	6.269	14.472	0.904
R4	0.754	6.268	14.472	1.326

The spectral accelerations calculated from the Loma Prieta earthquake recorded at the San Francisco International Airport are shown in Figure 6[7]. The fundamental periods of the fixed base model and two flexible base models are indicated on the figures. For comparison, the base shear coefficient in the UBC(1982) formula is presented, from which the design base shear was calculated. Depending on the value of natural period, response spectrum ordinates of the Loma Prieta earthquake are 2 to 5 times larger than the code coefficient. When the

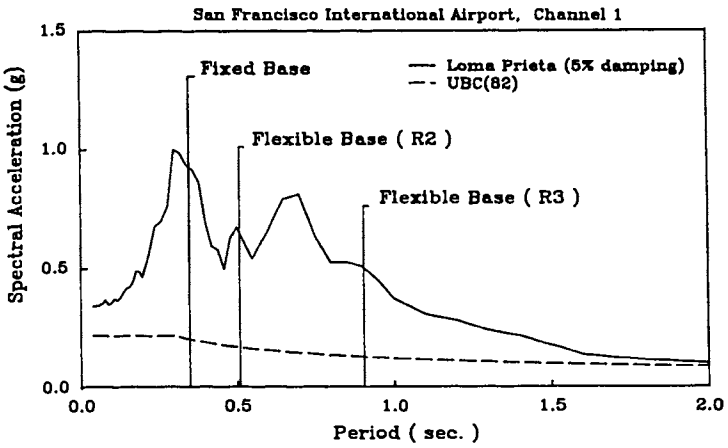

Fig. 6 Effect of Base Flexibility on Base Shear

building is subjected to strong ground motion, the building designed to resist code forces at working stress levels would experience inelastic deformations if there is no device or mechanism providing the required ductility and/or flexibility to keep the deformation of the building within the elastic range. Since the spectral acceleration of the Loma Prieta decreases rapidly at periods greater than 0.7 second, the lengthening of the fundamental period due to the foundation flexibility has a great effect on the base shear and base overturning moment.

Figure 7 shows the corresponding spectral displacements of the Loma Prieta earthquake. The periods of the three cases (fixed, R2, and R3) are marked on the figure, which shows the increase in displacements as the base becomes more flexible. It is noted that the spectral displacement curve is almost constant at periods greater than 0.9 second.

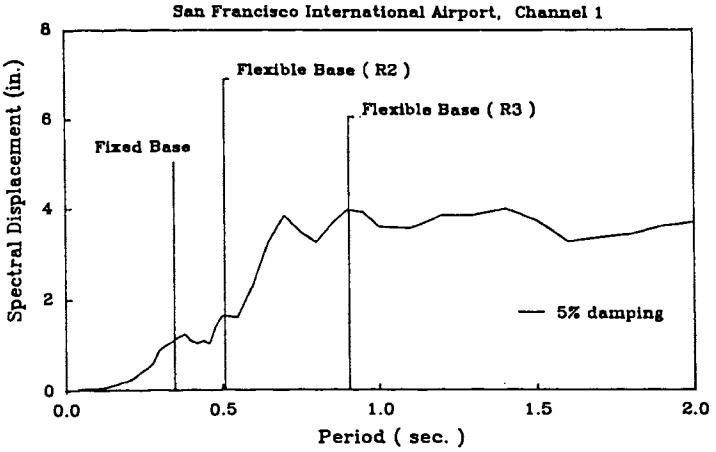

Fig. 7 Effect of Base Flexibility on Displacement

A nonlinear time history analysis is carried out with an assumed Rayleigh damping ratio of 5% for the superstructure and the pile. Figure 8 shows the Loma Prieta earthquake ground acceleration recorded at the San Francisco International Airport[7]. Figures 9~11 show time history plots of the horizontal roof displacement, base shear, and base overturning moment responses, respectively, for the fixed base and the flexible base(R3). The maximum responses are shown in Table 3 for the five base conditions. As the base rotation is released, the roof displacements and the rotations increase, but the inter-story drifts **decrease**. The reduction of the base shear is 25% for R1 and approaches 70% for R4, while the reduction of the base overturning moment is about 90% for R4. It is noted that the shear force at the pile head increases as the rotation at the base become more restricted.

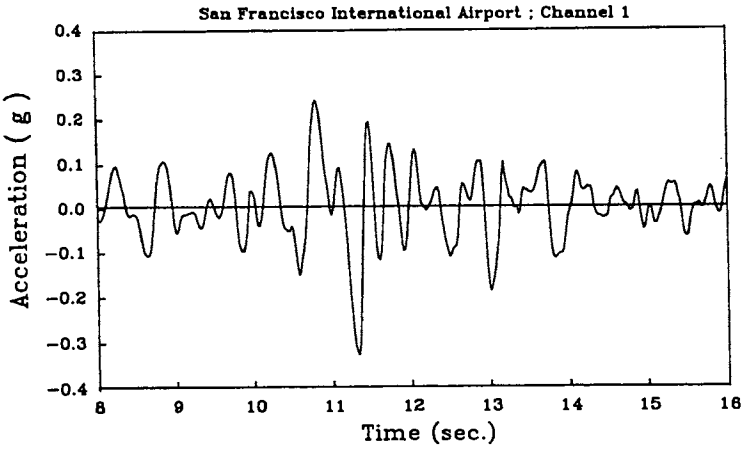

Fig. 8 Loma Prieta Earthquake

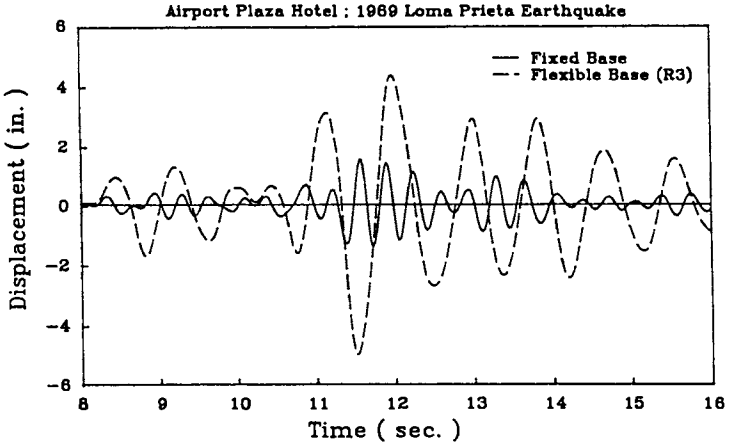

Fig. 9 Time History Plot of Roof Displacement

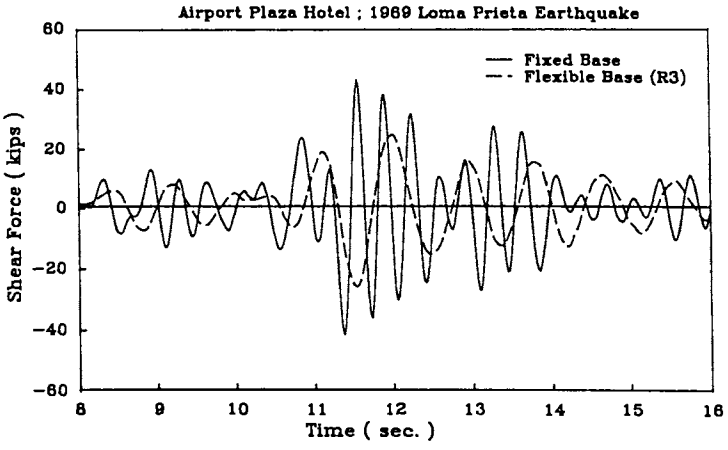

Fig. 10 Time History Plot of the Base Shear

Table 7 Maximum Responses of the Clarion Hotel under the Loma Prieta Earthquake

Response / Case	Fixed	R1	R2	R3	R4
Roof Displacement	1.549	1.265	1.905	5.037	4.717
Base Displacement		0.252	0.364	0.616	0.534
Roof Rotation	3.419	2.278	3.019	7.397	6.689
Base Rotation			1.034	6.238	6.653
Base Shear	42.606	31.693	32.102	27.148	12.475
Base Overturning Moment	1579.7	1062.6	1004.1	681.8	134.8
Shear Force at Pile Head		23.195	21.435	15.839	7.417
Moment at Pile Head		81.1	68.2	60.3	75.6

Unit : Displacement = in. , Moment = K ft , Shear Force = Kips

Fixed : Rotation at the base is fixed, no interaction.
R1 : Rotation at the base is fixed, interaction considered.
R2 : Rotational Spring Coefficient = 1.346E+7
R3 : Rotational Spring Coefficient = 1.346E+6
R4 : Rotational Spring Coefficient = 1.346E+5

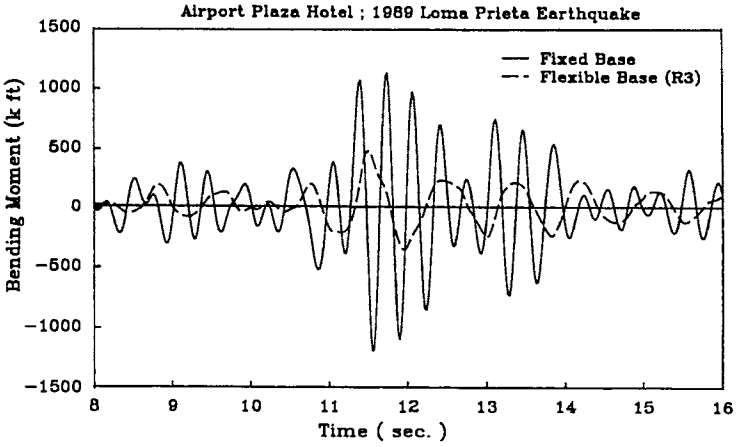

Fig. 11 Time History Plot of the Base Overturning Moment

As discussed above, the rotational resistance at the base has a pronounced effect on the responses of this particular structure. Thus, in order to estimate the responses correctly in the nonlinear analysis, it was necessary to calculate the coefficient of the rotational spring at the base in each loading step.

It is interesting to note that when the rotation at the base is fixed but interaction is still considered (R1), the roof displacement is smaller than that of the fixed base, which is similar to the responses of a base isolated structure using elastomeric rubber bearings as the isolator[8]. Of course the reductions calculated here are modest as compared to a base-isolated structure since the structure was not designed as much. Nevertheless, the potential for designing interactive pile foundation systems to function as isolators is evident.

It is also of interest to note that the roof displacements are significantly increased for the cases R3 and R4. Since the roof displacement is the total lateral structural movement relative to the ground, it is important to provide sufficient gap to avoid pounding between adjacent structures.

CONCLUSIONS

The influence of soil-pile-structure interaction on the response of a mid-rise reinforced concrete structure to the Loma Prieta earthquake was investigated. Tower I of the Clarion Hotel near San Francisco International Airport was studied in detail for five different base conditions. The analysis results show that the soil-pile-structure interaction has a significant effect on the response of the structure.

When the interaction is considered for Tower I of the Clarion Hotel, the natural period increased to 1.2 to 3.8 times longer than that of the fixed base structure as the rotational constraint at the base was decreased.

Because of the characteristics of the Loma Prieta earthquake and the period elongation through the soil-pile-structure interaction mechanism, the base shear and the base overturning moment are significantly reduced.

The roof displacement increases as the rotational constraint at the base becomes smaller. When the rotation at the base is completely fixed, the roof displacement is smaller than that of the fixed base, non-interactive case.

ACKNOWLEDGEMENT

The support of the National Science Foundation under the special Loma Prieta Earthquake Program is appreciated. Also the contribution of Dr. J. R. Harris, J. R. Harris & Co.,Structural Engineers and his associates, and the cooperation of the Clarion Hotel management are appreciated.

REFERENCES

Davisson, M.T. and Gill, H.L., "Laterally Loaded Piles in a Layered Soil System," J. Soil Mech. & Found. Div., ASCE, Vol. 89, No. SM3, May, 1963, pp. 63-84.

Reese, L.C. and Welch, R.C., "Lateral Loading of Deep Foundations in Stiff Clay," J. Geotech. Engng Div. ASCE, Vol. 101, No. GT7, 1975, pp.633-649.

Poulos, H.G. and Davis, E.H., Pile Foundation Analysis and Design, John Willey and Sons, Inc., New York, N. Y., 1980.

Pyke, R., "Nonlinear Soil Models for Irregular Cyclic Loadings," J. of Geotech. Engng. Div., ASCE, Vol.105, No.GT6, June, 1977, pp.715-726.

Hardin, B.O. and Drnevich, V.P., "Shear Modulus and Damping in Soils : design Equations and curves." J. Soil Mech. & Found. Div. ASCE, Vol. 98, No. SM7, July, 1972, pp.667-692.

Gazetas, G. and Dobry, R., "Horizontal Response of Piles in Layered Soils," J. Geotech. Engng Div. ASCE, Vol. 110, 1985, pp.20-40.

Huang et. al., Second Interim Set of CSMIP Processed Strong-Motion Records from the Santa Cruz Mountains (Loma Prieta) Earthquake of 17 October 1989, Report No. DSMS 90-01, Cal. Dept. Conservation, Feb. 1990.

"Comparison of Total Displacement," Seismic Isolation Update, Dynamic Isolation System Inc., Vol.4, No. 2, July 1990.